Smart/Micro Grids Research Center
smgrc

Energy Reports 6 (2020) 914–932

Contents lists available at ScienceDirect

Energy Reports

journal homepage: www.elsevier.com/locate/egyr

Research paper

A new stochastic gain adaptive energy management system for smart microgrids considering frequency responsive loads

Navid Rezaei [a,*], Mohammadreza Mazidi [b], Mehrdad Gholami [a], Maryam Mohiti [b]

[a] Department of Electrical Engineering, University of Kurdistan, Sanandaj, Iran
[b] Department of Electrical Engineering, Yazd University, Yazd, Iran

ARTICLE INFO

Article history:
Received 26 January 2020
Received in revised form 29 March 2020
Accepted 12 April 2020
Available online xxxx

Keywords:
Hierarchical control structure
Islanded microgrids
Droop gain scheduling
Frequency responsive loads
Two-stage stochastic optimization

ABSTRACT

Islanded microgrids as flexible, adaptive and sustainable smart cells of distribution power systems should be operated in accordance to both techno-economic purposes. Motivated by this need, the microgrid operators are in charge to elevate the active accommodation of both demand-side and supply-side distributed energy resources. To that end, in this paper, a new flexible frequency dependent energy management system is proposed through which distributed generators have time varying droop controllers with a gain-adaptive strategy. Besides to cope economically with uncertainty arise frequency excursions, a new, comfort-aware and versatile frequency dependent demand response program is mathematically formulated and conducted to the energy management system. It is aimed to co-optimize the microgrid energy resources such a way the day-ahead operational costs are managed subject to a secure frequency control portfolio. The presented model is solved using a two-stage stochastic programming and by a tractable efficient mixed integer linear programming approach. The simulation results are derived in 24-h scheduling time horizon and implemented on a typical test microgrid. The effectiveness of the proposed hourly gain assignment and frequency responsive load management program has been verified thoroughly by analyzing the results.

1. Introduction

1.1. Motivation and needs

An Islanded Microgrid (IMG) can be defined as an adaptable and sustainable block in distribution power systems which assemble versatile demand-side and supply-side distributed energy resources (DER) to procure energy demands with high security and flexibility (Rezaei and Kalantar, 2015b). The microgrid central controller (MGCC) main task is to reliably preserve the load balance constraint while at the same time all the required techno-economic targets of a smart microgrid are tailored (Rezaei and Kalantar, 2015b; Guerrero et al., 2013). Similar to large scale power systems, one of the great challenges of the IMGs is to manage the frequency excursions arise from operational uncertainties in a secure and economic portfolio (Rezaei and Kalantar, 2015b; Simpson-Porco et al., 2017). The MGCC should provide a flexible framework to adapt with uncertainties and frequency restrictions by optimal coordinating both droop controlled distributed generations (DGs) and demand response programs (Bidram and Davoudi, 2012; Eid et al., 2014). Motivated by this need, in this paper, a new frequency aware adaptable energy management system is proposed which can be folded in two main contributions. First, a new, comfortable, economic and highly flexible frequency responsive demand response program is established and mathematically modeled. The constructed frequency responsive load (FLR) model is based on potential of thermostatically controlled loads in providing discretized step-wise set-point modification in response to system frequency feedbacks. Next, the droop controllers of the DGs are changed to an adaptive time varying blocks through which an optimal hourly gain assignment strategy is conducted according to the system operational feedbacks. In gist, the paper concentrates on an adaptive energy management system aims to manage the day-ahead operational costs subject to secure control of stochastic frequency excursions. To cope with uncertainties of load consumption and renewable energy sources (RES) a two-stage stochastic programming is adopted and the whole optimization model is solved by an effective tractable mixed integer linear programming approach. The executed high accommodate IMG energy management system can procure imperative cost-effective frequency control paradigm by flexible coordination of the droop gains and FLR set-point modifications.

* Corresponding author.
E-mail address: n.rezaei@uok.ac.ir (N. Rezaei).

https://doi.org/10.1016/j.egyr.2020.04.021

Nomenclature

Indices

$h \in H$	Index of hours
$s \in S$	Index of scenarios
$g \in G$	Index of distributed generators
$i \in I$	Index of photovoltaic units
$w \in W$	Index wind turbine units
$n \in N$	Index of natural responsive loads
$d \in D$	Index of demand response providers

Parameters

B	Natural load frequency dependency coefficient
VLL	Value of Lost Load
π	Probability of scenario
f^0	Nominal frequency of MG
$\overline{\Delta f}$	Maximum allowable microgrid frequency excursion limit
α	Fixed operation cost of DG
β	First-order operation cost of DG
δ	Start-up/shut-down cost of DG
ρ^{DRP}	The cost associated to demand response providers
λ^{WT}	The operation cost of WT
λ^{Pv}	The operation cost of PV
$\overline{P^{DG}}$	Maximum power generation of DG
$\underline{P^{DG}}$	Minimum power generation of DG
$\overline{UR^{DG}}$	Ramp-up limit of DG
DR^{DG}	Ramp-down limit of DG
UT^{DG}	Minimum up-time limitation of DG
DT^{DG}	Minimum down-time limitation of DG
P^{L}	Forecasted load consumption of MG
$\overline{P^{WT}}$	Maximum forecasted power output of WT
$\overline{P^{PV}}$	Maximum forecasted power output of PV

Variables

P^{DG_ref}	Active power reference of DG
P^{DG_ref}	Power output of DG
n^{gain}	Droop gain of DG
f^{MG}	Frequency of MG
ΔP^{L}	Load deviation from its forecasted
ΔP^{WT}	WT power deviation from its forecasted
ΔP^{PV}	PV power deviation from its forecasted
ΔP^{DG}	Power deviation of DG from its reference
ΔP^{NR}	Power deviation associated to natural responsive loads
ΔP^{FR}	Power deviation associated to frequency responsive loads
LSH	Involuntary load shedding
u	Binary variable indicating commitment state of DG
u^{ON}	Binary variable indicating start-up state of DG
u^{OFF}	Binary variable indicating the shut-down state of DG

1.2. Literature review

To provide a background of the research this section is allocated to review the associated literature. In some papers, frequency excursions arising from the uncertainties in the environment of IMGs are ignored and energy management is only conducted to optimize operation objectives. In Marzband et al. (2013), a real-time control system is proposed to operate and validate the hybrid resources in the IMGs, experimentally. In Zia et al. (2019), a determinist EMS is proposed for an IMG that optimizes both the operating and emission costs. In Marzband et al. (2017) a multi-period optimization algorithm is implemented for economic scheduling of IMGs. Moreover, an artificial neural network is used to predict uncertainties. In Singh et al. (2018), an EMS is proposed for IMGs to regulate voltage through optimal control of electric vehicles. In Pourghasem et al. (2019), a stochastic multi-objective model for optimal management of combined heat and power based IMGs is proposed considering the uncertainties of forecasted wind power and load demand. Another stochastic EMS is proposed in Farzin et al. (2017) to minimize total operation cost during unscheduled MG islanding periods using optimal scheduling of all resources. Authors of Liu et al. (2016) has proposed an optimal scheduling model for minimizing the operating costs of an IMG by using chance-constrained programming approach. A stochastic frequency security constrained EMS for an isolated MG with droop controlled DGs is proposed in Rezaei and Kalantar (2014). A new technical objective function is extended. It minimizes frequency deviations during day-ahead MG operation and limits operational and emission costs of MG to a reasonable level. In Vahedipour-Dahraie et al. (2017), a two-stage stochastic model for optimal frequency-security constrained energy and reserve scheduling in an IMG is proposed. The droop coefficients are considered fixed. In Rezaei et al. (2018), a robust EMS based on information gap decision theory is proposed for IMGs to minimize operation cost while managing frequency excursions. Authors of Gholami and Sun (2018) have proposed a framework for minimizing total load shedding cost of MGs while the frequency stability is ensured following unplanned contingencies. In Rezaei and Kalantar (2015a), a multi-objective EMS is proposed for IMGs in which optimal prices of energy and frequency security is determined for droop-controlled DGs.

In the above papers the droop coefficients are permanently allocated on the basis of the capacity of the controllable DGs. However, with the advent and installation of Advanced Measurement Infrastructure (AMI) in the smart MGs, there is the possibility of adaptive optimizing droop coefficients depending on time and operation set-point. In Li et al. (2016), an agent-based distributed model is proposed to control the frequency and perform economic dispatch of an IMG with renewable resources. In Abdelaziz et al. (2014), a probabilistic algorithm is used to optimally adjust the droop gains of DGs considering uncertainties of renewable generations and loads. In Ref. Khaledian et al. (2017), a two-layer real time energy management is proposed to reduce the frequency deviation and provide an economic power sharing between DGs in an IMG. Optimal droop gain assignment of DGs based on combination of gradient descent method and minimum mean square frequency error strategy is used in the second layer. Although the variable droop coefficients are considered for DGs, the effects of uncertainty of the renewable resources and loads are not considered. A similar model is proposed in Abedini and Abedini (2018) to optimize droop parameters of

DGs aims to improve voltage and frequency excursions of IMGs with minimum cost. In Abdelaziz and El-Saadany (2015), a probabilistic analytical control strategy is proposed to optimally select the droop gains of DGs in order to minimize the uncertainties. In Aunedi et al. (2013), a frequency related demand response model based on refrigeration appliances through an advanced stochastic control strategy is proposed for frequency regulation under renewable uncertainties. Plug in electric vehicles (PEVs) is used as another demand side response to improve primary frequency control. Regarding to the fast response of PEVs in comparison to conventional DGs, some portions of PEVs reserve is replaced by DGs by using a new control strategy after a certain time (Izadkhast et al., 2017). Table 1, summarizes the comparison between the proposed model and other existing approaches. As it can be interpreted no research can be found, to the best of our knowledge, which is comprehensively manage the microgrid operational uncertainties using coordinated scheduling of the gain adaptive droop controllers and thermostatically based frequency responsive loads. Besides, the proposed step-wise model of frequency responsive loads is new, comfort-preserving, economic and provocative for both the end-user demand response providers and the MGCC. The conducted frequency dependent unit commitment model is transformed into a tractable and high efficient linear one which implements an effective new linearization lemma to convert bilinear bounded variables that can be used easily by commercial solvers. In other words, the present paper fulfills the gap of providing a linearized EMS for frequency management of IMGs by joint time-dependent gain assignment of the droop controllers and optimal daily load scheduling in a cost effective manner.

1.3. Paper contributions

In gist, the objective of the proposed EMS is to minimize total operation cost of the IMG while its frequency security is guaranteed in a cost-effective manner. To this end, the MGCC manages the gains of the droop controlled DGs in coordination with frequency-responsive loads while all techno-economic constraints of the IMG are ensured, simultaneously. Moreover, to promote the proposed EMS, droop gain of controllable DGs are models as time dependent variables and adaptively optimized in such a way that the frequency security of the MG, along with the objective function based on its economy, is fulfilled. To cope with the enforced operational uncertainties, the proposed EMS model is formulated as a two-stage stochastic mixed-integer linear programming (MILP) problem that guaranties achieving the global optimal solution. In the following, the main contributions of the paper are highlighted:

- Proposing a novel energy management system for IMGs including precise modeling of the droop controlled DGs and frequency-responsive loads in which all techno-economic constraints of MG are ensured.
- Modeling droop gain of controllable DGs as time dependent variables which are adaptively optimized in response to the system hourly new set-points.
- Introducing a new mathematical model of frequency responsive loads based on the behavior of thermostat controlled loads.
- Coordinating time-varying gain assignment of controllable DGs with frequency responsive loads to increase the cost-effectiveness of the proposed frequency aware EMS.
- Utilizing a new, effective and tractable mixed-integer linear programming formulation that guaranties achieving the global optimal solution.

1.4. Paper organization

The reminder of this paper is organized as follows. In Section 2, the uncertainty modeling of WT power generation, PV power generation, and load are presented. The frequency responsive load model is introduced in Section 3. Then, problem formulation and description are presented in Section 4. Numerical study is performed in Section 5 and finally, the conclusion is provided in Section 6.

2. Uncertainty modeling

Different uncertainties related to forecasted power generation of WTs and PVs as well as MG load demand should be considered in the proposed gain adaptive EMS which are modeled in this section by probability distribution functions (PDFs). Moreover, an efficient scenario generation and reduction method are introduced to reduce the computational burden.

2.1. Wind power generation

The Weibull distribution as a typical PDF fits wind speed variations with high precision, hence it is used to model wind speed uncertainty (Wang and Gooi, 2011). The PDF of Weibull distribution is as follows:

$$f(v) = \left(\frac{k}{c}\right)\left(\frac{v}{c}\right)^{k-1} exp\left[-\left(\frac{v}{c}\right)^{k-1}\right] \tag{1}$$

The power generation of WTs is a function of wind speed and is presented as follows:

$$P_w^{WT} = \begin{cases} 0; & 0 \le v \le Vci_w \\ P_w^{rated} \times \dfrac{(v - Vci_w)}{(Vr_w - Vci_w)}; & Vci_w \le v \le Vr_w \\ P_{rated}; & Vr_w \le v \le Vco_w \\ 0; & Vco_w \le v \end{cases} \tag{2}$$

where, P^{rated}, v, Vci, Vr, and Vco are the rated power, forecasted wind speed, cut-in speed, rated speed and cut-off speed of WT, respectively.

2.2. Photovoltaic generation

The variations of solar irradiance at a particular location usually follow a Beta distribution which is used to model the solar irradiance uncertainty (Mazidi et al., 2014). The PDF of Beta distribution is as follows:

$$f(I) = \begin{cases} \dfrac{\Gamma(\alpha+\beta)}{\Gamma(\alpha)\Gamma(\beta)} I^{(\alpha-1)}[1-I]^{(\beta-1)}; & 0 \le I \le 1 \\ 0; & otherwise \end{cases} \tag{3}$$

The parameters of Beta distribution can be calculated using the mean and standard deviation of uncertain variable, i.e., solar irradiance, as follows:

$$\beta = (1-\mu_I) \times \left(\frac{\mu_I(1+\mu_I)}{\sigma_I^2} - 1\right) \tag{4}$$

$$\alpha = \frac{\mu_I \times \beta}{1-\mu_I} \tag{5}$$

The irradiance-to-power conversion function is used to calculated the power generation of PVs:

$$P_i^{PV} = \eta_i^{PV} \times S_i^{PV} \times I; \quad 0 < I < \infty \tag{6}$$

where, I, η^{PV}, and S^{PV} are the solar irradiation, efficiency (%), and total area (m^2) of PV, respectively.

Table 1
Comparison of the proposed model with the existing approaches.

Ref	Frequency-responsive loads	Day-ahead adaptive droop gains	Frequency security margins	Load uncertainty	Renewable generation uncertainty	Economic based energy management system	Linearized microgrid unit-commitment model	Stochastic programming
Marzband et al. (2017)						×		
Singh et al. (2018)							×	
Pourghasem et al. (2019)				×	×			
Farzin et al. (2017)		×						
Liu et al. (2016)				×	×			×
Rezaei and Kalantar (2014)				×	×	×	×	×
Vahedipour-Dahraie et al. (2017)				×	×	×	×	
Rezaei et al. (2018)			×	×	×		×	×
Gholami and Sun (2018)			×	×	×	×	×	×
Rezaei and Kalantar (2015a)			×	×	×	×	×	
Li et al. (2016)			×	×	×			
Abdelaziz et al. (2014)			×	×	×	×	×	×
Khaledian et al. (2017)		×	×			×	×	
Abedini and Abedini (2018)		×		×	×	×	×	
Abdelaziz and El-Saadany (2015) and Aunedi et al. (2013)		×	×			×		
Izadkhast et al. (2017)		×	×			×		
Wang and Gooi (2011)	×				×	×		×
Mazidi et al. (2014)	×					×		
This paper	×	×	×	×	×	×	×	×

2.3. Load demand

The load uncertainty is modeled with normal distribution which its PDF is as follows (Wang and Gooi, 2011):

$$f(P_L) = \frac{1}{\sqrt{2\pi\sigma_L^2}} exp\left(-(P_L-\mu_L)^2/\left(2\sigma_L^2\right)\right) \tag{7}$$

where, P_L is load demand of MG with mean value and standard deviation of μ_L and σ_L, respectively.

2.4. Scenario generation and reduction

The forecasted uncertainties associated with power generation of WTs and PVs as well as MG load demand are modeled by continuous PDFs in the previous subsections. However, using the PDFs in the continuous format makes the optimization problem very complicated. Therefore, the continuous PDF of each uncertain variable is divided into discrete intervals to form multiple states and then combined, to generate a scenario set. As shown in Fig. 1, the relative PDFs which are used for modeling the uncertainty in wind speed, solar irradiation, and load demand of MG are divided to 5, 5, and 7 discrete intervals, respectively. Note that the considered intervals are an example of discretizing the continuous PDFs, it can also be divided into more discrete intervals in accordance to the desired preciseness. It should be mentioned that each state represents an expected value for the uncertain variable with its occurrence probability. The expected value is considered as the middle of the interval while its probability can be easily calculated by integration.

To combine the different discrete PDFs, the scenario tree is used in this paper (Mazidi et al., 2019; Zakariazadeh et al., 2014). As can be seen in Fig. 2, each scenario includes three different states of wind power, solar power, and MG load at each hour of scheduling horizon. Likewise, a weight π_s is assigned to each scenario that indicates the probability of its occurrence.

$$S_s = \left\{d_i, w_j, p_k\right\}; \forall s = 1, 2, \ldots, N \tag{8}$$

$$\pi_s = \pi_{d_i} \times \pi_{w_j} \times \pi_{p_k}; s = 1, 2, \ldots, N \tag{9}$$

Accordingly, if the relative PDFs which are used for modeling the uncertainty in wind speed, solar irradiation, and load demand of MG are divided to 5, 5, and 7 discrete intervals, $N = N_i \times N_j \times N_k = 175$ scenarios would be generated at each hour of scheduling.

As the large number of scenarios makes the optimization problem insolvable, a scenario reduction method should be applied. To select the desired scenarios (NS) form the first N generated scenarios by scenario tree method, a stopping criterion is defined as (10) and applied to the generated scenarios of each hour, then the NS remained scenarios selected as the reduced desired scenarios and transferred to the next hour. The procedure is iterated over the whole 24 h scheduling period. The stopping criterion is based on standard deviation of the solved scenarios in each hour. That is, the normalized standard deviation with respect to the mean value after solving the proposed optimization problem over each generated scenario is computed and compared to a pre-specified threshold (Wu et al., 2007; Amjady et al., 2009). The given threshold can be various according to the preciseness of the problem and can be chosen from 0.01 to 0.05. In this paper, the threshold of the stopping criterion is set at 0.03, hence the remained scenarios (NS) from the employed scenario reduction methodology is set on 20.

$$\sigma_n = \frac{1}{NS.\mu}\sqrt{\sum_{s=1}^{NS}\frac{(ESF_s-\mu)}{NS-1}} \tag{10}$$

where, σ_n is the normalized standard deviation of the ESF objective function in the accepted scenarios. ESF_s is the optimized value of the objective function in scenario s. − is the mean value of the ESF in scenario s.

The proposed scenario reduction approach explained which is based on the simultaneous backward algorithm (Growe-Kuska et al., 2003). The backward reduction method for large scenario reduction is included in the SCENRED library. This scenario reduction algorithm provided by SCENRED determine a scenario subset (of prescribed cardinality or accuracy) and assign optimal probabilities to the preserved scenarios (GAMS, 0000).

3. Frequency responsive load modeling

The loads which participate in MG frequency management can be categorized in two cases, namely, natural response loads and frequency controlled loads (responsive loads). These loads are modeled in the following of this section.

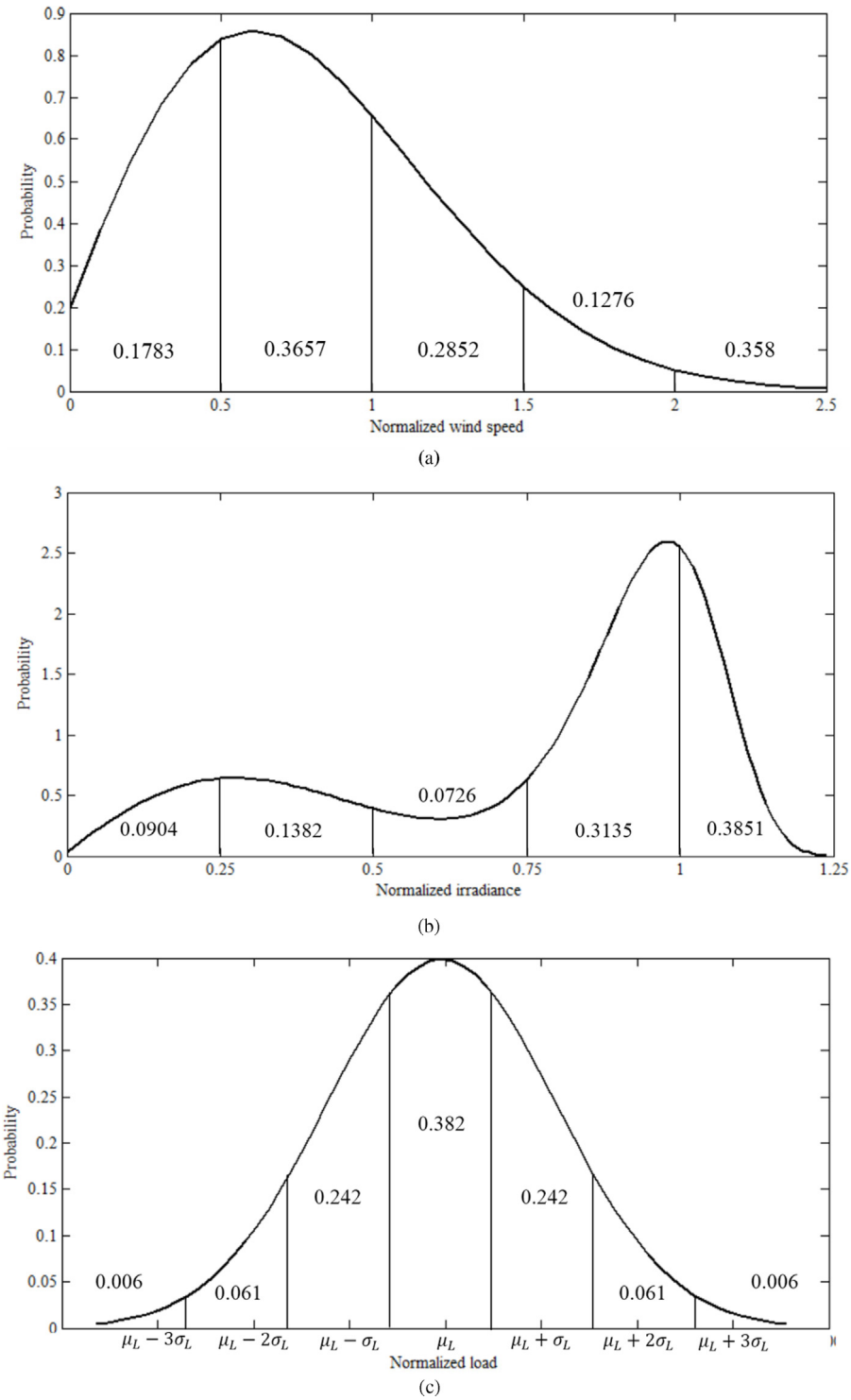

Fig. 1. Probability distribution function of (a) wind speed, (b) solar irradiation, and (c) load demand of MG (Mazidi et al., 2019).

3.1. Natural response load

In natural response loads the demand changes as the frequency changes according to the nature of the load. For example, in induction machines, the machine slows down when the frequency drops, which leads to lessened power demand (Elizondo et al., 2016). The amount of power variation can be written as a function of frequency variation for natural response loads (NRLs) (Samarakoon et al., 2012):

$$\Delta P^{NR}_{s,n,h} = B_{n,h}\Delta f_{s,h} \tag{11}$$

where, $B_{n,h}$ is a coefficient which depends on the natural frequency of the load which can be determined experimentally according to the type and technical characteristics of different loads. In this paper, it is assumed that NRLs are elastic with respect to the frequency of MG. Thus, $B_{n,h}$ can be calculated as follows:

$$B_{n,h} = \frac{P^{NR}_{n,h}}{f^0} \tag{12}$$

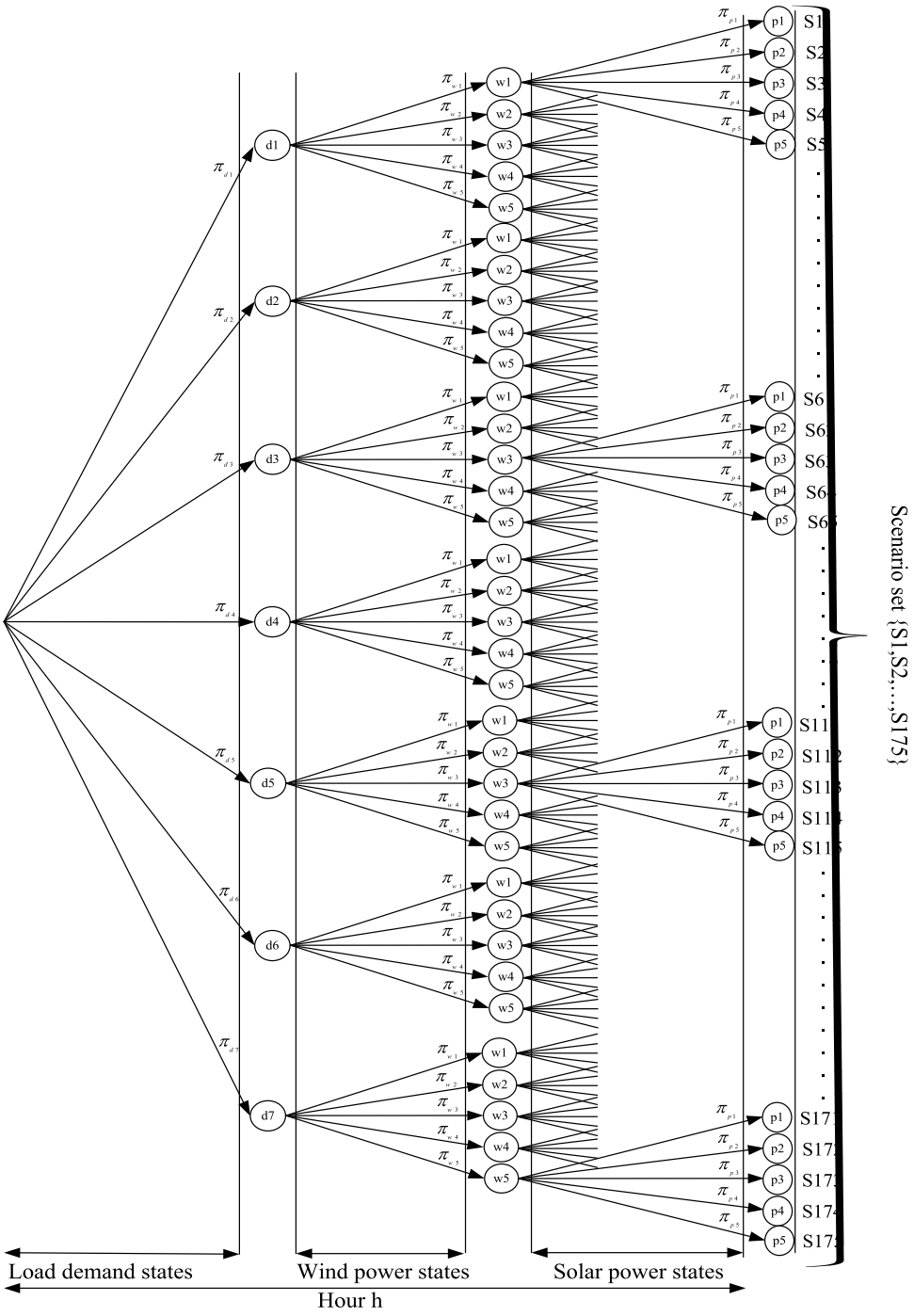

Fig. 2. Scenario tree for combination of wind power, solar power, and load forecasted values.

3.2. Frequency responsive load

Thermostat controlled loads with fast controller such as refrigerators, freezers, air conditioners and electric water and space heaters can be utilized as frequency responsive loads (FRLs). In these loads, the power consumption could be controlled as a function of the frequency (Molina-Garcia et al., 2011; Xu et al., 2011). To this end, the set-points of FRLs are adjusted with respect to the frequency excursion:

$$T_h^{Set} = \begin{cases} T_h^{Set0} + K^{FRL}\left(f_h - f^0\right); & f > \bar{f} \\ T_h^{Set0}; & \underline{f} < f < \bar{f} \\ T_h^{Set0} - K^{FRL}\left(f^0 - f_h\right); & f < \underline{f} \end{cases} \tag{13}$$

According to (13), when the frequency exceeds the upper bound, the desired set points increase which leads to turning on thermostat loads. On the other hand, when the frequency excursion exceeds the lower bound, the desired set points decrease and consequently thermostat loads are turned off. This concept is shown in Fig. 3.

It should be mentioned that the desired temperature of FRLs should be preserved in a pre-specified range which is implied by the following constraint (Ghofrani et al., 2019):

$$\underline{T^{Set}} \le T_h^{Set} \le \overline{T^{Set}} \tag{14}$$

Although utilization FRLs to manage frequency excursion is an effective solution, but controlling a large number of them is

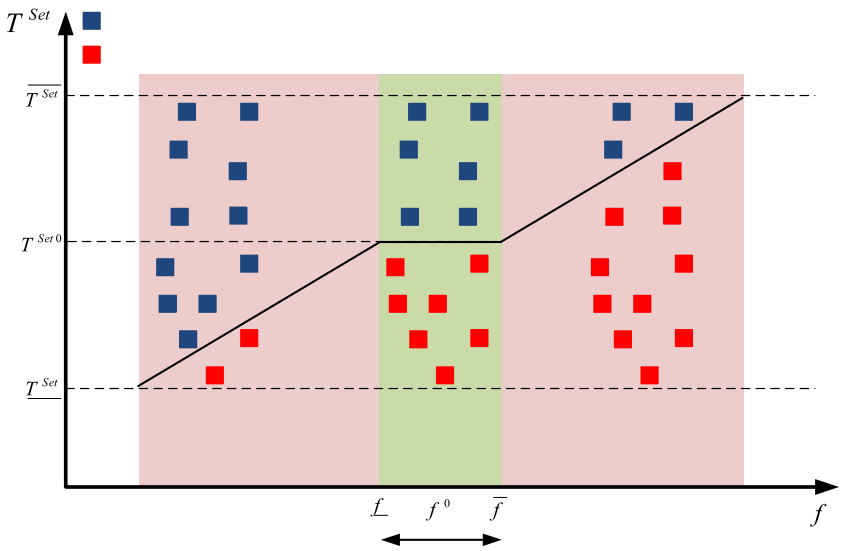

Fig. 3. Control of thermostat loads to manage variation of system frequency.

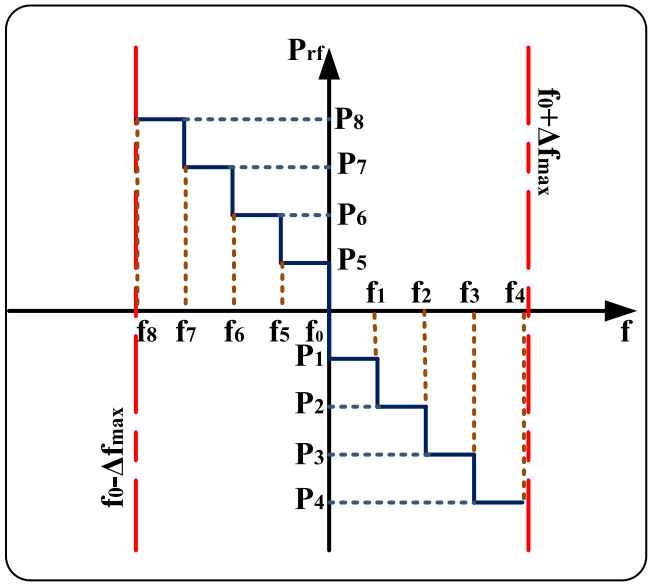

Fig. 4. Step-wise power–frequency packages.

a challenging task. To cope with this issue, demand response providers (DRPs) register the FRLs, aggregate their power, and submit the aggregated power–frequency function on behalf of them to the EMS. It is assumed that the submitted power–frequency function of DRPs are in form of step-wise power–frequency packages which are shown in Fig. 4.

The above shown step-wise power–frequency packages could be formulated as follows:

$$\Delta P^{FR}_{s,d,h} = \begin{cases} -P_{J-j+1}; & f^0 \le f^{MG}_{s,h} \le f^0 + \overline{\Delta f} \quad \forall j \in J \\ P_i; & f^0 - \overline{\Delta f} \le f^{MG}_{s,h} \le f^0 \quad \forall i \in I \end{cases} \tag{15}$$

where, j and i are indexes for the number of divisions in the interval of $[f^0, f_0 + \overline{\Delta f}]$ and the number of controllers of the interval of $[f^0 - \overline{\Delta f}, f^0]$, respectively. They are adjusted using a frequency dependent controller. It should be noted the consumer comfort index should be considered for the entire settings.

4. Model description and formulation

The structure of the proposed gain adaptive EMS for a typical IMG is shown in Fig. 5. As can be seen, the EMS includes two control levels, i.e., primary and secondary. The aim of primary control level is to compensate the frequency excursions and provide a stable balance between the generation and demand in the IMG. The second control level has the most important role in the proposed EMS which is performed by the MGCC in a centralized manner. In the following of this section, each control level is explained in details with corresponding mathematical formulations and then the proposed EMS is presented.

4.1. Primary control level

The primary controllers compensate the frequency excursions caused by the variability of renewable generation resources as well as MG load fluctuations based on the characteristics of the droop-controlled DGs in a distributed and automatic manner. As mentioned, the inertia of VSI based DGs is much smaller than a synchronous generator. Therefore, to mimic the governor of a synchronous generator, a virtual inertia is added to VSI based DGs using an active power–frequency (P/f) droop which is shown in Fig. 6 and described as follows (Raj et al., 2018):

$$f_{s,h} = f^0 + n^{gain}_{g,h}\left(P^{DG\_ref}_{g,h} - P^{DG}_{s,g,h}\right); \forall s, g, h \tag{16}$$

According to (16), when the MG takes positive frequency excursions, the generation power of controllable DGs are decreased to alleviate the frequency excursions while the generation power of controllable DGs are increased for the sake of mitigation the negative frequency excursion.

Primary control level guarantees that all of controllable DGs generate voltages with the same steady state angular frequency (Abdelaziz et al., 2012). Thus, the frequency of IMG can be calculated as follows:

$$\begin{aligned} f^{MG}_{s,h} &= f^0 + n^{gain}_{1,h}\left(P^{DG\_ref}_{g=1,h} - P^{DG}_{s,g=1,h}\right) \\ &= f^0 + n^{gain}_{g=2,h}\left(P^{DG\_ref}_{g=2,h} - P^{DG}_{s,g=2,h}\right) \\ &= \cdots = f^0 + n^{gain}_{g=G,h}\left(P^{DG_{ref}}_{g=G,h} - P^{DG}_{s,g=G,h}\right); \forall s, h \end{aligned} \tag{17}$$

It should be mentioned that the droop, i.e., n^{gain}, and the reference of active power, i.e., P^{ref}, of controllable DGs are fixed at each

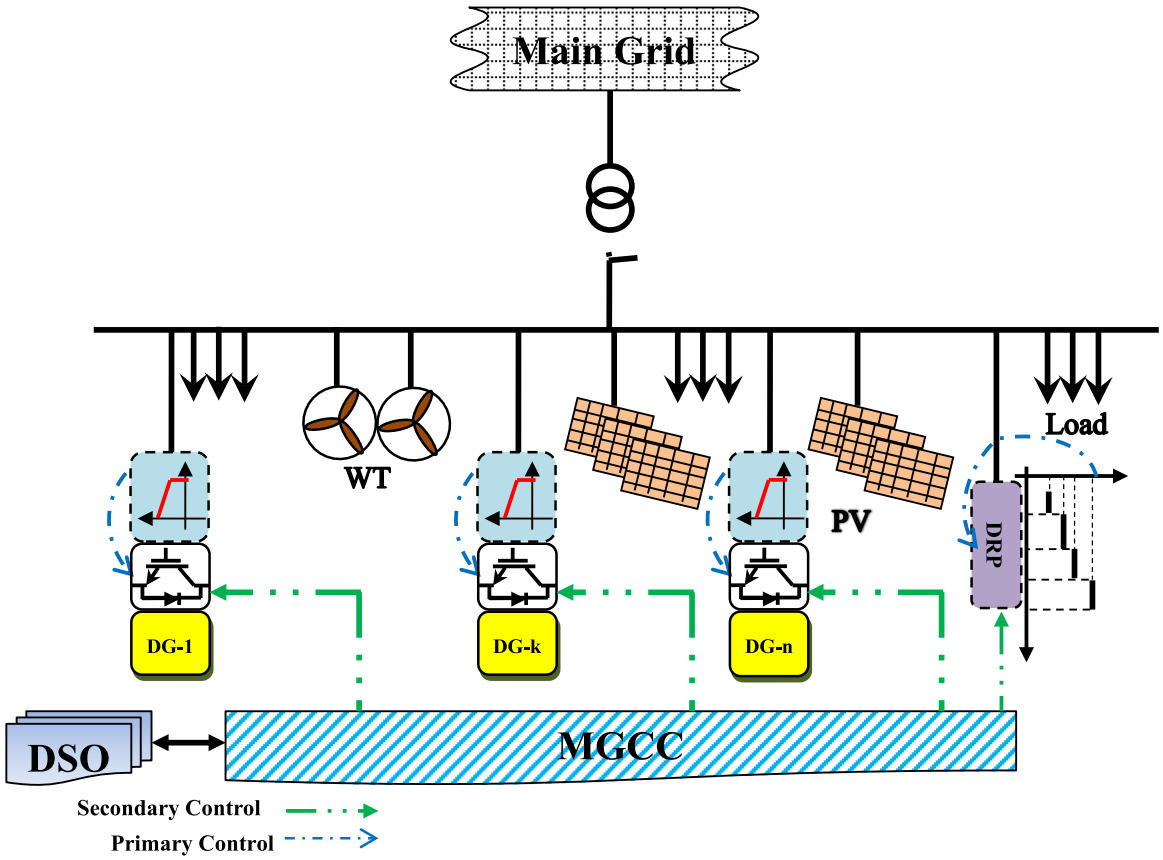

Fig. 5. The structure of the proposed EMS.

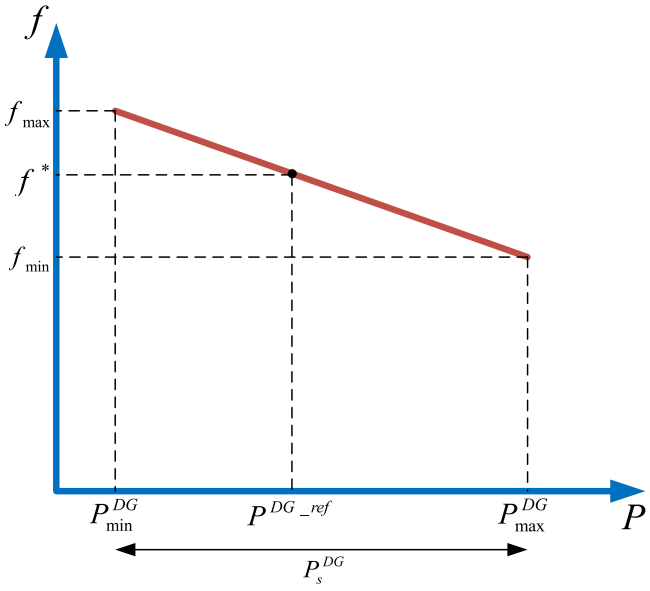

Fig. 6. Active power–frequency (P/f) droop characteristic.

hour of scheduling horizon by the value determined by the MGCC. In fact, the main contribution of this paper is to determine the optimal values of n^{gain} and P^{ref} for controllable DGs of the MG in a way that not only the operation cost is minimized but also the MG frequency lies within the secure ranges. This concept is shown in Fig. 7. As can be seen, if the values of n^{gain} and P^{ref} are optimally adjusted, following a greater variation in renewable generation resources or load, the frequency of MG can be preserved within a pre-defined secure range.

4.2. Secondary control level

The MGCC lies on the second control level and plays an important role in the proposed EMS. Indeed, the MGCC is responsible for optimal operation of the IMG subject to all techno-economic constraints. To this end, the MGCC locally determines active power references of droop-controlled DGs and their droop gains as well as responsiveness level of FRLs such that not only the operation cost is minimized but also the MG frequency lies within the secure ranges. In the following the objective function and constraints of the second control level are formulated.

4.2.1. Objective function

The objective of MGCC is modeled by a stochastic optimization function as follows:

$$\begin{aligned} Minimize\ F = \sum_{h=1}^{H} \Bigg[\sum_{g=1}^{G} \Big[\Big(\alpha_g u_{g,h} + \beta_g P_{g,h}^{DG\_ref} \Big) \\ + \delta_g \times \left(u_{g,h}^{ON} + u_{g,h}^{OFF} \right) \Big] \\ + \sum_{w=1}^{W} \lambda_w^{WT} P_{w,h}^{WT} + \sum_{i=1}^{I} \lambda_i^{PV} P_{i,h}^{PV} \end{aligned}$$

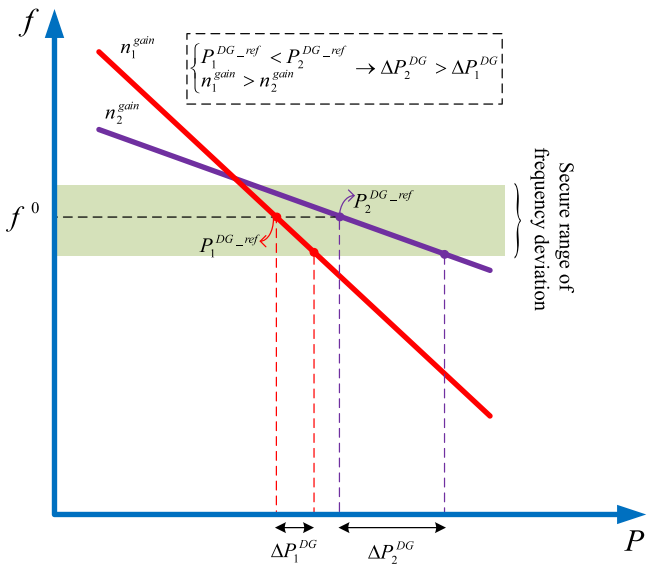

Fig. 7. Impact of droop gain and power reference on frequency security of IMG.

$$+\sum_{s=1}^{S}\pi_s\times\left[\sum_{g=1}^{G}\beta_g\Delta P_{s,g,h}^{DG}+\sum_{w=1}^{W}\lambda_w^{WT}\Delta P_{s,w,h}^{WT}+\sum_{i=1}^{I}\lambda_i^{PV}\Delta P_{s,i,h}^{PV}+\sum_{d=1}^{D}\rho_d^{DRP}\Delta P_{s,d,h}^{FR}+VLL\times LSH_{s,h}\right] \quad (18)$$

According to the objective function, the first part implies the fuel cost, start-up cost, and shut down cost of controllable DGs as well as operation cost of WTs and PVs. This part associates with the first-stage decisions and does not rely on scenarios. The second part shows the scenario-related part of the objective function and depends on the second stage decisions. It includes some terms that reflect the power deviation costs of controllable DGs, WTs, and PVs from their scheduling, deployed cost of frequency responsive loads, and load shedding which should be paid for the damages inflicted to the customers due to an electric power interruption.

4.2.2. Constraints

The following technical and economic constraints should be considered in the second control layer of the proposed EMS:

Power balance: At each hour of scheduling horizon, supplied power from the committed DGs and renewable resources must satisfy the load demand of MG:

$$\sum_{g=1}^{G}P_{g,h}^{DG\_ref}u_{g,h}+\sum_{w=1}^{W}P_{w,h}^{WT}+\sum_{i=1}^{i}P_{i,h}^{PV}=P_h^L;\forall h \quad (19)$$

Following the power variations of renewable resources and loads from their forecasted values, power generation of controllable DGs and responsive level of FRLs should be adjusted in a way that the active power balance is always satisfied during scheduling horizon. Otherwise, an unplanned load shedding is unavoidable. Accordingly, the following constraint is enforced:

$$\sum_{g=1}^{G}\Delta P_{s,g,h}^{DG}u_{g,h}+\sum_{w=1}^{W}\Delta P_{s,w,h}^{WT}+\sum_{i=1}^{i}\Delta P_{s,i,h}^{PV}=\Delta P_{s,h}^{L}-\sum_{n=1}^{N}\Delta P_{s,n,h}^{NR}-\sum_{d=1}^{D}\Delta P_{s,d,h}^{FR}-LSH_{s,h};\forall s,h \quad (20)$$

It should be mentioned that with power variations of renewable resources and loads, the frequency of IMG deviates from its nominal value; Therefore, the consumption of NRLs changes which is also considered in (20). Meanwhile, the amount of load shedding should be less than total MG load which is imposed by the following constraint:

$$0\le LSH_{s,h}\le P_{s,h}^{L} \quad (21)$$

Controllable DGs: To guarantee the safe operation of controllable DGs the following constraints should be considered (Mazidi et al., 2016):

$$\underline{P_g^{DG}}u_{g,h}\le P_{g,h}^{DG\_ref}\le\overline{P_g^{DG}}u_{g,h};\forall g,h \quad (22)$$

$$P_{g,h}^{DG\_ref}-P_{g,h-1}^{DG\_ref}\le UR_g^{DG}\left(1-u_{g,h}^{ON}\right)+\underline{P_g^{DG}}u_{g,h}^{ON};\forall g,h \quad (23)$$

$$P_{g,h-1}^{DG\_ref}-P_{g,h}^{DG\_ref}\le DR_g^{DG}\left(1-u_{g,h}^{OFF}\right)+\underline{P_g^{DG}}u_{g,h}^{OFF};\forall g,h \quad (24)$$

$$\sum_{t=1}^{h+UT_g^{DG}-1}u_{g,t}\ge UT_g^{DG}u_{g,h}^{ON};\forall g,h \quad (25)$$

$$\sum_{t=1}^{h+DT_g^{DG}-1}\left(1-u_{g,t}\right)\ge DT_g^{DG}u_{g,h}^{OFF};\forall g,h \quad (26)$$

$$u_{g,h+1}-u_{g,h}\le u_{g,h+1}^{ON};\forall g,h \quad (27)$$

$$u_{g,h}-u_{g,h+1}\le u_{g,h+1}^{OFF};\forall g,h \quad (28)$$

$$u_{g,h+1}-u_{g,h}\le u_{g,h+1}^{ON}-u_{g,h+1}^{OFF};\forall g,h \quad (29)$$

The capacity limit of DGs is given by (22). Constraints (23) and (24) represent the ramp up and ramp down capabilities of DGs, respectively. Moreover, the minimum up time and down time of DGs are considered in (25) and (26), respectively. To prevent conflicted situations in the status of DGs, constraints (27) to (29) are incorporated.

The constraints related to safe operation of DGs at each scenario should also be satisfied:

$$\underline{P_g^{DG}}u_{g,h}\le P_{s,g,h}^{DG}\le\overline{P_g^{DG}}u_{g,h};\forall s,g,h \quad (30)$$

$$P_{s,g,h}^{DG}-P_{s,g,h-1}^{DG}\le UR_g^{DG}\left(1-u_{g,h}^{ON}\right)+\underline{P_g^{DG}}u_{g,h}^{ON};\forall s,g,h \quad (31)$$

$$P_{s,g,h-1}^{DG}-P_{s,g,h}^{DG}\le DR_g^{DG}\left(1-u_{g,h}^{OFF}\right)+\underline{P_g^{DG}}u_{g,h}^{OFF};\forall s,g,h \quad (32)$$

Frequency security: The variation of renewable power generation and load from their forecasted values causes the frequency of IMG to deviate from the nominal frequency. Therefore, the security constraint of the MG should be considered as follows:

$$\left|\Delta f_{s,h}\right|\le\overline{\Delta f};\forall s,h \quad (33)$$

where,

$$\left|\Delta f_{s,h}\right|=\left|f_{s,h}^{MG}-f^0\right|;\forall s,h \quad (34)$$

Droop constraint: According to (17), the following constraint should be considered by the MGCC for calculating the optimal values of droop gains:

$$n_{g=1,h}^{gain}\Delta P_{s,g=1,h}^{DG}=n_{g=2,h}^{gain}\Delta P_{s,g=2,h}^{DG}=\cdots=n_{g=G,h}^{gain}\Delta P_{s,g=G,h}^{DG};\forall s,h \quad (35)$$

where,

$$\Delta P_{s,g,h}^{DG}=P_{s,g,h}^{DG}-P_{g,h}^{DG_{ref}};\forall s,g,h \quad (36)$$

Note that according to (33), the frequency deviations of MG should be preserved within a pre-defined secure range. Therefore, the following constraint is needed to be considered by the MGCC in calculating the optimal values of n^{gain}:

$$0 \le n_{g,h}^{gain} \le \overline{n_g^{gain}} u_{g,h} = \frac{\overline{\Delta f}}{\overline{P_g^{DG}}} u_{g,h}; \forall g, h \tag{37}$$

Renewable resources: The scheduling power of WTs and PVs must always be smaller than their maximum power generations:

$$P_{s,w,h}^{WT} \le \overline{P_{s,w,h}^{WT}}; \forall s, w, h \tag{38}$$

$$P_{s,v,h}^{PV} \le \overline{P_{s,v,h}^{PV}}; \forall s, v, h \tag{39}$$

It should be mentioned that the constraints of (22) to (29) should be only considered for controllable DGs.

4.3. Linearization

Microgrid energy management system is inherently laid out as high constrained non-linear and usually with non-convex region. To reach the optimal solution, the MGCC can utilize either evolutionary or classic optimization algorithms. Each strategy has its own advantages, however, in the case of evolutionary optimization techniques, the decision making process may suffer from difficult constraint handling and large computational time in such non-linear and highly constrained optimization problem the MGCC confronted in the microgrid energy management system. Thus, conducting mathematical classic optimization portfolios such nonlinear programming can fulfill the drawbacks of the constraint handling and/or computation speed in some ways. However, in nonlinear programming based solvers, guaranteeing the solution optimality may be unreliable. Hence, the linear programming which ensure reaching to the nearest global optimal solution by relying on efficient simplifying assumption may be more attractive from the MGCC.

In order to implement a linear programming approach, the nonlinear terms namely, (34) and (35), should be modified into their equivalent linear formats. The linear expression of (34) can be illustrated by the following substitutions (Rezaei and Kalantar, 2014):

$$\left|\Delta f_{s,h}\right| = \Delta f_{s,h}^{+} + \Delta f_{s,h}^{-}; \forall s, h \tag{40}$$

$$\Delta f_{s,h} = \Delta f_{s,h}^{+} - \Delta f_{s,h}^{-}; \forall s, h \tag{41}$$

$$\Delta f_{s,h}^{+} \ge 0, \Delta f_{s,h}^{-} \ge 0; \forall s, h \tag{42}$$

Constraint (35) establishes a non-linear relationship between power variations of controllable DGs. This non-linearity can be converted into linear expressions by employing the McCormick lemma (Gupte et al., 2013). In general form, bilinear term $M_k.N_l$ in which continuous variables are bounded as $M_k^{min} \le M_k \le M_k^{max}$ and $N_l^{min} \le N_l \le N_l^{max}$ can be recast using a relaxation replacement including a new variable H_{kl} by some adjoined constraints as follows in Equation set (43) (Ghofrani et al., 2019):

$$\begin{aligned}
&\left(M_k - M_k^{min}\right)\left(N_l - N_l^{min}\right) \ge 0 \rightarrow H_{kl} - N_l^{min} M_k - M_k^{min} N_l \\
&\qquad + M_k^{min} N_l^{min} \ge 0 \\
&\left(M_k - M_k^{min}\right)\left(N_l^{max} - N_l\right) \ge 0 \rightarrow -H_{kl} + N_l^{max} M_k \\
&\qquad + M_k^{min} N_l - M_k^{min} N_l^{max} \ge 0 \\
&\left(M_k^{max} - M_k\right)\left(N_l - N_l^{min}\right) \ge 0 \rightarrow -H_{kl} + N_l^{min} M_k \\
&\qquad + M_k^{max} N_l - M_k^{max} N_l^{min} \ge 0 \\
&\left(M_k^{max} - M_k\right)\left(N_l^{max} - N_l\right) \ge 0 \rightarrow H_{kl} - N_l^{max} M_k - M_k^{max} N_l \\
&\qquad + M_k^{max} N_l^{max} \ge 0
\end{aligned} \tag{43}$$

Table 2
Economic data of controllable DGs.

DG	α ($)	β ($/kWh)	SUC ($)	SDC ($)
MTs	85.06	4.37	9	8
FCs	255.18	2.84	16	9
GT	212.00	3.12	12	8

Table 3
Technical data of controllable DGs.

DG	P^{min} (kW)	P^{max} (kW)	RMP^{up}/RMP^{dn} (kW)	ST^{up}/SH^{dn} (kW)	T^{MUP}/T^{MDN} (h)
MTs	30	150	250	100	2
FCs	20	100	250	100	2
GT	35	200	280	120	2

To this end, in this paper, each term $n_{g,h}^{gain} \Delta P_{s,g,h}^{DG}$ is replaced by an added new continuous variable $X_{s,g,h}$ and adjoined by the following constraints:

$$X_{s,g,h} \ge 0; \forall s, g, h \tag{44}$$

$$-X_{s,g,h} + \overline{P_g^{DG}} \times n_{g,h}^{gain} \ge 0; \forall s, g, h \tag{45}$$

$$-X_{s,g,h} + \overline{n_g^{gain}} \times \Delta P_{s,g,h}^{DG} \ge 0; \forall s, g, h \tag{46}$$

$$X_{s,g,h} + \overline{n_g^{gain}} \times \overline{P_g^{DG}} - \overline{n_g^{gain}} \times \Delta P_{s,g,h}^{DG} - \overline{P_g^{DG}} \times n_{g,h}^{gain} \ge 0; \forall s, g, h \tag{47}$$

Using the above expressions, the proposed gain adaptive energy management system can be solved using an efficient mixed-integer linear programming methodology in which the global optimal solution is guaranteed.

5. Numerical study

5.1. Data

To evaluate the effectiveness of the proposed gain adaptive energy management system, it is implemented for an IMG test system which is shown in Fig. 8. The MG has five droop controlled DGs including two micro-turbines (MTs), two fuel cells (FCs), and a gas turbine. Meanwhile, two WTs and two PVs has been installed in the MG. Both the natural and frequency responsive loads are connected to the MG and a DRP is considered for managing all the frequency responsive loads. The economic and technical data of controllable DGs are taken from Rezaei and Kalantar (2015b) and Rezaei and Kalantar (2014) and presented in Tables 2 and 3, respectively. The WTs are the same type with the parameters of P_{rated} = 100 kW, Vci = 2.5 m/s, Vr = 10 m/s and Vco = 20 m/s. Meanwhile, the PVs are also the same type with the parameters of η^{PV} = 12% and S^{PV} = 500 m^2. The operation cost of WTs and PVs, i.e. λ_w^{WT} and λ_i^{PV}, are assumed to be 1 cent/kW and 0.8 cent/kW, respectively (Zhang et al., 2017). It is assumed that all the DGs and renewable resources are operating at unity power factor and reactive power requirements have been technically guaranteed.

The hourly forecasted values of solar irradiance, wind speed, and MG load demand over 24-h time interval are retrieved from Mazidi et al. (2019) which are illustrated in Fig. 9. The parameters of Weibull distribution are assumed $c = v/0.9$ and $k = 2$ for all hours (Wang and Gooi, 2011). Meanwhile the standard deviations of solar irradiance and MG load demand are assumed 10% and 20% of their forecasted, respectively.

It is assumed that 10 NRLs are connected to the MG which contain 10% of MG load demand at each hour of scheduling horizon. In the step-wise power–frequency package of DRP, 8 same steps

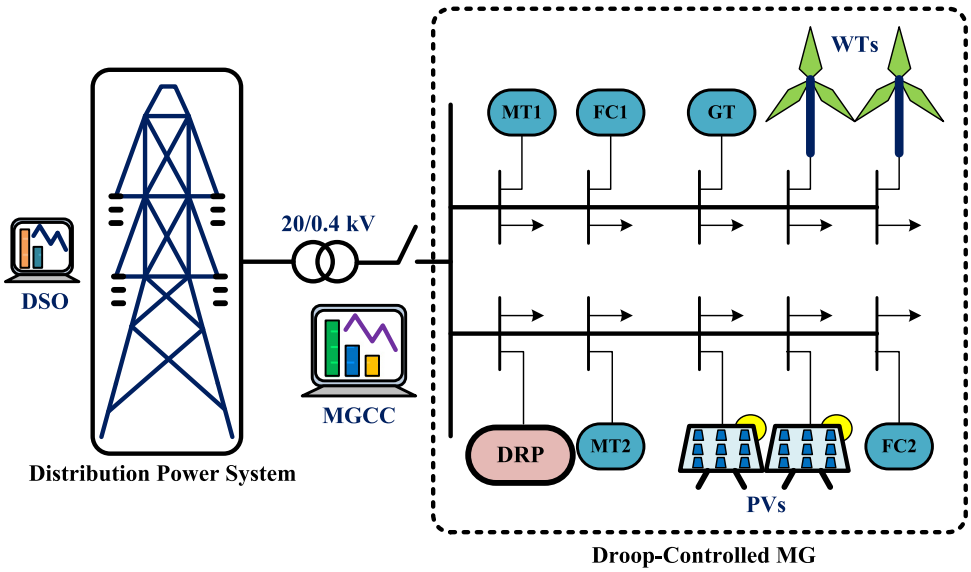

Fig. 8. Microgrid test system equipped with its components.

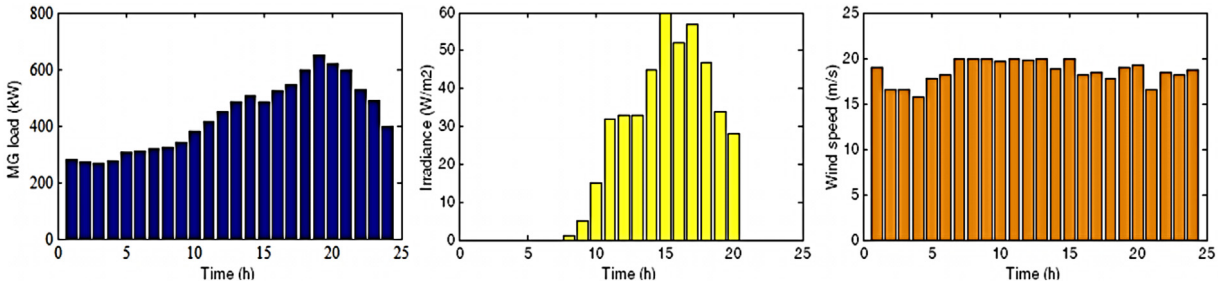

Fig. 9. Hourly forecasted of load, solar irradiance, and wind speed.

with values of 40 kW and 37.5 mHz are considered for power and frequency, respectively. Meanwhile, the cost associated to the DRP is set 100 $/kWh. Based on the IEEE Std-1547 (Anon, 2014), the maximum permissible frequency deviation is set to ±300 mHz. Meanwhile, the nominal frequency of the MG is considered to be 60 Hz. Meanwhile, the VLL is taken 1000 $/kWh.

The proposed EMS is a MILP problem that was solved using CPLEX 12.5.1 under GAMS (GAMS, 0000) on a 3.60-GHz Intel Core i7 CPU personal computer with 8 GB of RAM memory. The gap tolerance for solving MILP problem was 0.05%.

5.2. Results and discussion

To model the uncertainties related to power generation of WTs and PVs as well as load demand of MG, 175 scenarios are generated using scenario tree method and then, reduced to 20 by SCENRED tool which is provided by GAMS. The active power deviations of WT, PV as well as load demand of MG over the 24-h time interval are generated for different scenarios which are shown in Figs. 10, 11, and 12, respectively.

The energy management for the 24-h time interval is performed for the test MG, and the optimal values for reference power of controllable DGs and theirs droop gains as well as responsiveness level of frequency-dependent loads are obtained. The hourly power reference of controllable DGs is shown in Fig. 13. As can be seen, the DGs with lower operation cost, e.g., DG5, are the most dispatchable units. Meanwhile, although DG1 and DG2 have the highest operation cost, but they have been dispatched during the scheduling horizon. The reason is that dispatching DG1 and DG2 increases the capability of the MG to preserve frequency deviations within the permissible secure range. In other words, according to the optimal droop gains of DG1 and DG2, they can participate in balancing between generation and demand of the MG following deviations of WT, PV as well as load from their forecasted values. This strategy leads to the lowest operation cost while the frequency security is respected during the scheduling horizon.

Table 4
Maximum droop gain of controllable DGs.

DG	DG1	DG2	DG3	DG4	DG5
$\overline{n_g^{gain}}$ (kW/Hz)	500	500	333	333	666

The optimal gains are obtained adaptively in the proposed EMS for different scenarios which are presented in Fig. 14. As can be seen, during the hours in which the power deviations of WTs, PVs as well as load from their forecasted values increases, namely between 15 to 24, the gains of controllable DGs are increased. In this way, the capability of DGs in compensation of power deviations increases which leads to keep the frequency of MG in the pre-defined secure range. The values of maximum droop gain can be calculated using (35) which are presented in Table 4. Note that the droop gain of controllable DGs are always lower than the maximum allowable gains during the scheduling horizon.

Fig. 15. represents the responsiveness level of FRLs which are aggregated by the DRP in each scenario during scheduling horizon of the MG. The MGCC uses the capability of FRLs besides the controllable DGs to preserve the frequency deviations of MG in a secure range in a way that operation cost is minimized. As can be

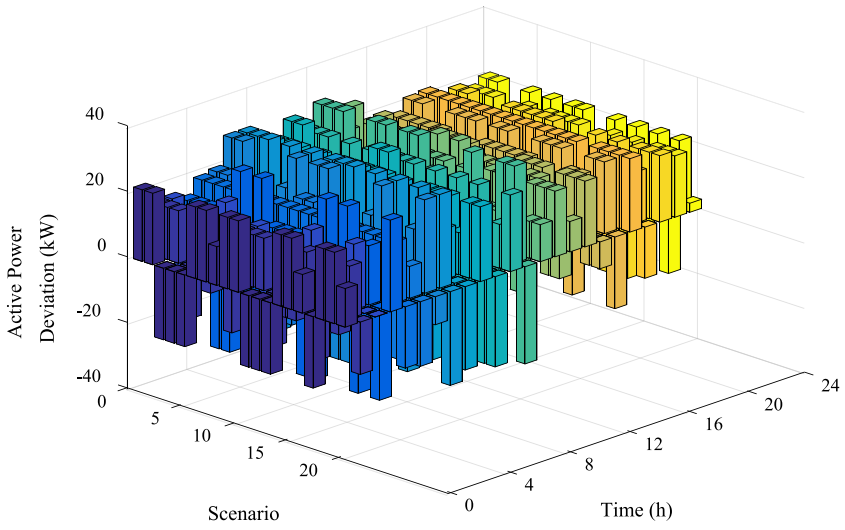

Fig. 10. WT active power deviations in each scenario.

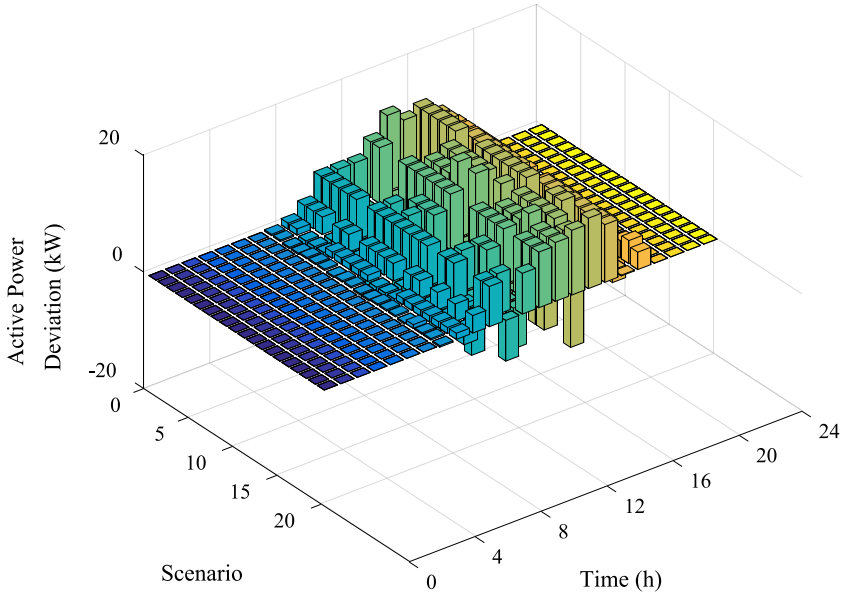

Fig. 11. PV active power deviations in each scenario.

seen, DRP is mostly called to reduce the consumption of FRLs during the hours 1 to 12 of the scheduling horizon. This is due to the fact that during these hours, reference power of controllable DGs is relatively low which reduces their capability in compensation of frequency deviations. However, with increasing the reference power of controllable DGs, the participation of DRP reduces and the MGCC prefers to use capability of controllable DGs in the frequency management of the DG. These strategies reduce the operation cost of the MG during the scheduling horizon.

Another option that is considered in the scheduling horizon of the MG is the load shedding, which is shown in Fig. 16 for each scenarios during scheduling horizon. As can be seen, the values of load shedding are zero in most of the scenarios. In fact, due to high penalty cost which has to be paid for the damages inflicted to the customers, the MGCC schedules controllable DGs and FRLs to compensate frequency deviations. However, in some scenarios, namely hours 1 and 6, power deviations of WTs, PVs as well as load from their forecasted values cannot be compensated completely by the controllable DGs and FRLs and therefore, the MGCC forces to shed loads.

Fig. 17 shows the frequency deviations of the MG in each scenario during scheduling horizon. As can be seen, the frequency deviations are successfully limited within secure range of ± 300 mHz. To this end, the MGCC has scheduled the controllable DGs and FRLs which leads to higher operation cost. The expected frequency excursion and expected operation cost of the MG over scenarios are shown in Fig. 18. As can be seen, with increasing the frequency excursion, the operation cost increases. On the other hand, with reducing the frequency excursion, the operation cost relatively reduces. This is due to the fact that the MGCC schedules the controllable DGs and FRLs with a higher operation cost to cope with frequency excursions during the scheduling horizon. It should be mentioned that this is the cost relating to the MG frequency insurance.

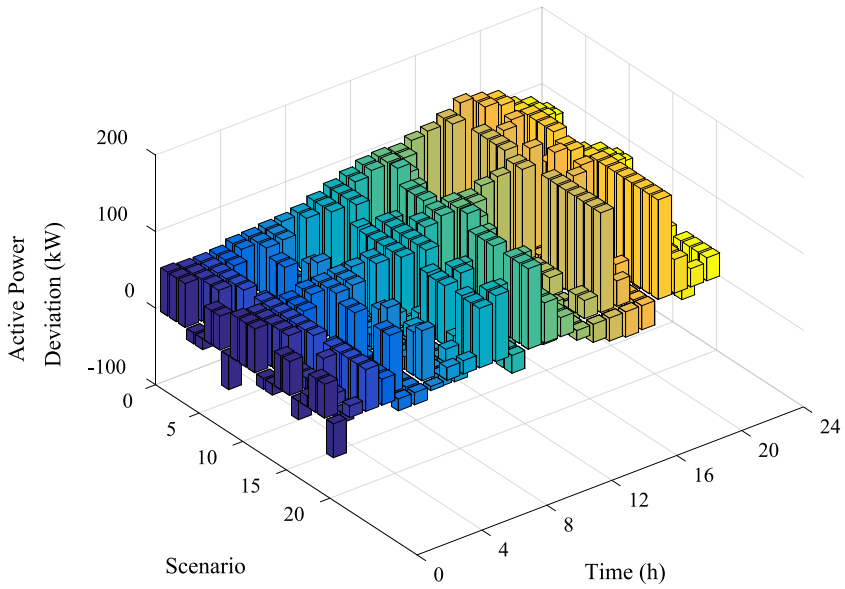

Fig. 12. MG load demand power deviations in each scenario.

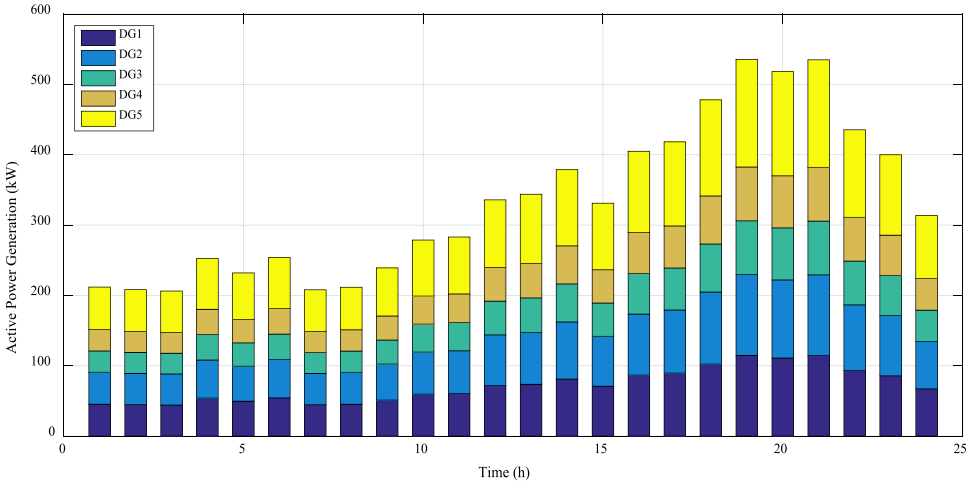

Fig. 13. Optimal power references of controllable DGs.

5.3. Discussion

For the sake of a detailed analysis, the optimization results in scenario 6 over 24 h of scheduling horizon are evaluated. These results are presented in Table 5. As can be seen, the frequency of the MG becomes 59.78 and 60.12 Hz at hours 7 and 16, respectively. This is due to the fact that power deviations of WTs, PVs and load from their forecasted values cause generation shortage at hour 7 and generation excess at hour 16. To cope with this issue, primary controller increases the generation power of controllable DGs at hour 7 while the generation power of controllable DGs are decreased at hour 16. Meanwhile, the MGCC calls the DRP to reduce power of FRLs by 21.08 kW at hour 7 and increase 2.64 at hour 16. Accordingly, the balance between power supply and load demand in the MG is improved. Note that the demand of NRLs are reduced by 1.34 kW at hour 7 and increased by 1.1 at hour 16. Likewise, the MGCC enforces to shed 16.7 kW at hour 7 to balance between power supply and load demand in the MG.

To increase the reliability of the proposed model, the load shedding in each scenario can be limited to a predefined value. Fig. 19 represents the expected frequency of the MG with respect to maximum allowable load shedding. As expected, with decreasing the maximum allowable load shedding, the expected frequency of the MG is reduced. In other words, the frequency security of the MG is increased. However, this issue increases the operation cost of the MG as shown in Fig. 20. The reason is that, MGCC schedules more controllable DGs and FRLs to preserve the balance between power supply and load demand during the scheduling horizon.

The given threshold can be various according to the preciseness of the problem and can be chosen from 0.01 to 0.05. In this paper, the threshold of the stopping criterion is set at 0.03, hence the remained scenarios (NS) from the employed scenario reduction methodology is set on 20 in this paper. Too few scenarios may cause inaccurate results, while too many scenarios may make the problem computationally impractical. Fig. 21 illustrates the evolution of expected cost versus different stopping criteria,

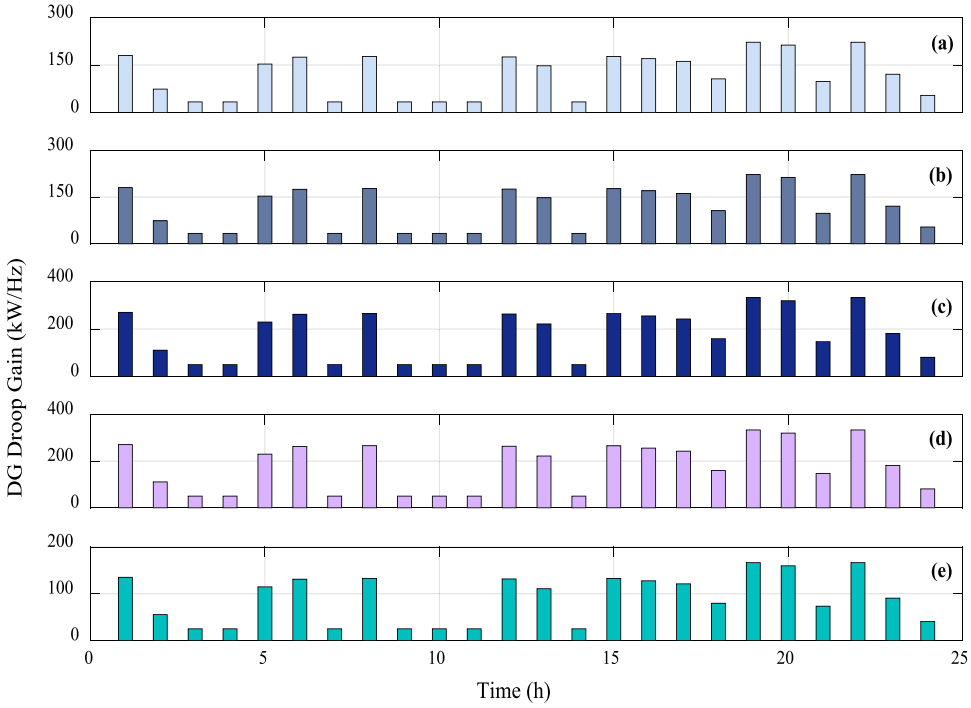

Fig. 14. Scheduled droop gains: (a) DG1, (b) DG2, (c) DG3, (d) DG4, (e) DG5.

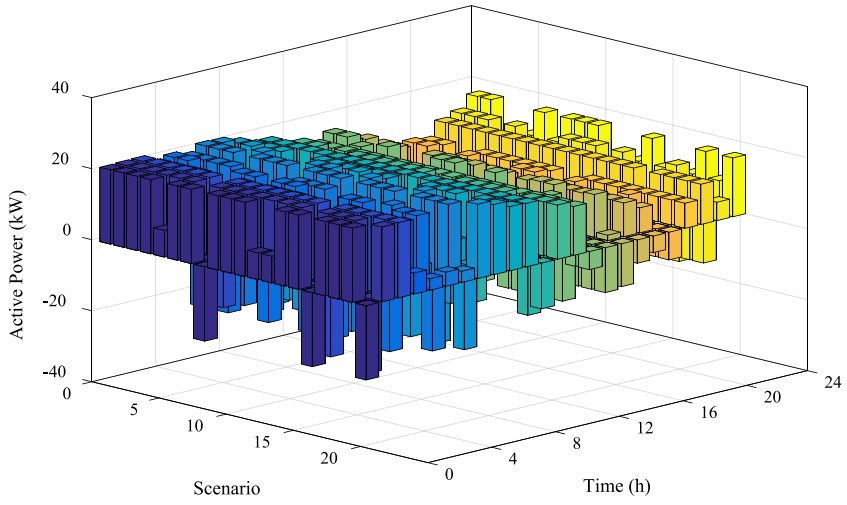

Fig. 15. The responsiveness level of FRLs.

i.e., σ_n. As can be seen, the expected cost fixes in vicinity of 0.03 which indicates 20 scenarios. Thus, accuracy of the results obtained in this paper is ensured.

To provide a verification portfolio in this section, a Monte-Carlo Simulation (MCS) strategy is employed to compare with the adopted stochastic programming approach. In the executed MCS, 1000 random scenarios are generated considering to the operational uncertainties are generated. The statistical histogram and the fitted normal probability distribution function is depicted in Fig. 20. The maximum, minimum, mean and standard deviation values of the MG cost function derived out by running the MCS are 293494.87$, 141599$, 190576.41$ and 40018.67$, respectively. The optimal solution of the stochastic programming approach is 219001.08$ which can be considered as a reasonable optimal solution with respect to the statistical values of the MCS based histogram. In other words, as can be seen from Fig. 20, the MG operational cost optimized using the scenario-based stochastic programming framework conducted over 20 reduced efficient scenarios is neither a conservative nor an opportunistic solution. It is median optimistic solution with reasonable distance with respect to the mean and max values resulted by applying the MCS over 1000 random scenarios. This helps the MGCC to rely on the stochastic programming solution which has less computational burden, provides efficient covering of the MG uncertainty spectrum through a non-conservative optimality achievement (see Fig. 22).

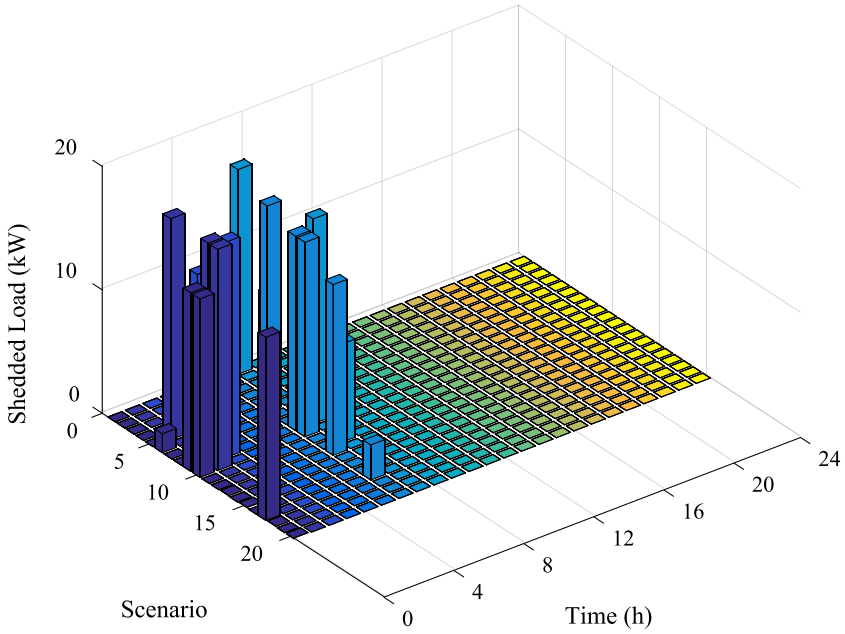

Fig. 16. MG load shedding in each scenario.

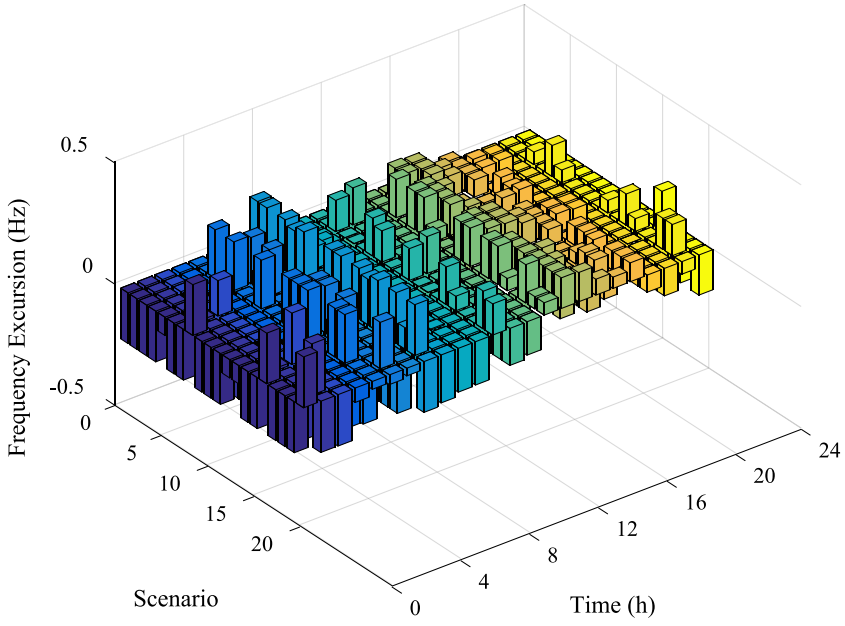

Fig. 17. MG frequency deviations in each scenario.

6. Conclusion

In contrast to conventional energy management systems, where MGs frequency deviations are not taken into account, this paper proposed a novel gain adaptive energy management system for IMGs operation considering frequency responsive loads. The proposed gain adaptive scheme brought out high flexibility, reliability and sustainability for the smart microgrids. To cope with the enforced operational uncertainties, the proposed EMS model is formulated as a two-stage stochastic MILP problem that guaranties achieving the near-optimal solution. The operational uncertainties were managed effectively by coordinated utilization of demand-side and supply-side energy providers which can guarantee the renewable sources sustainable integration even with higher penetration levels. Simulation results demonstrated that by proper scheduling droop controlled DGs and FRLs, the frequency of the IMG can be cost-effectively preserved within a pre-defined secure range under enforced operational uncertainties. Note that the proposed EMS model increases the operation cost of the IMG to ensures the MG frequency security. This is the cost relating to the MG frequency insurance. Moreover, it is shown that by increasing the reliability of the proposed EMS model, the frequency security of the IMG is improved which increases the operation cost. Furthermore, optimal operational cost

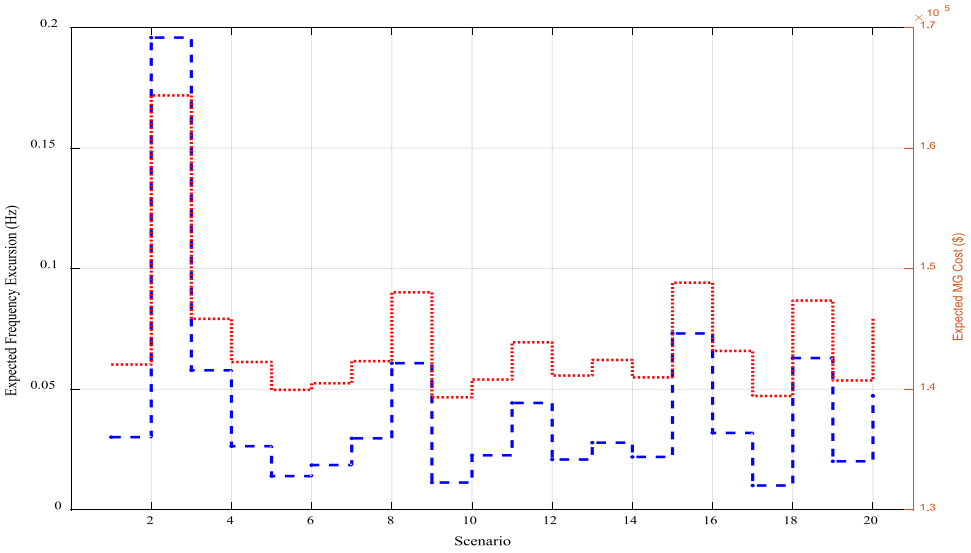

Fig. 18. Expected frequency excursion and operational cost of MG.

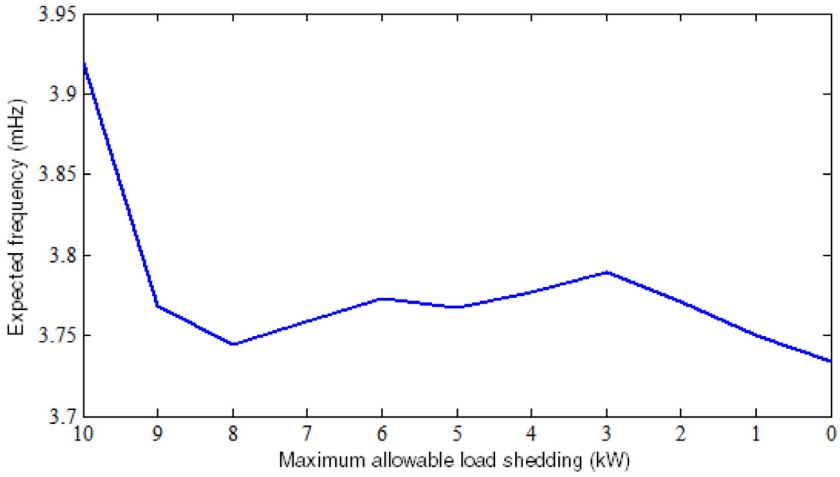

Fig. 19. Expected frequency of MG with respect to maximum allowable load shedding.

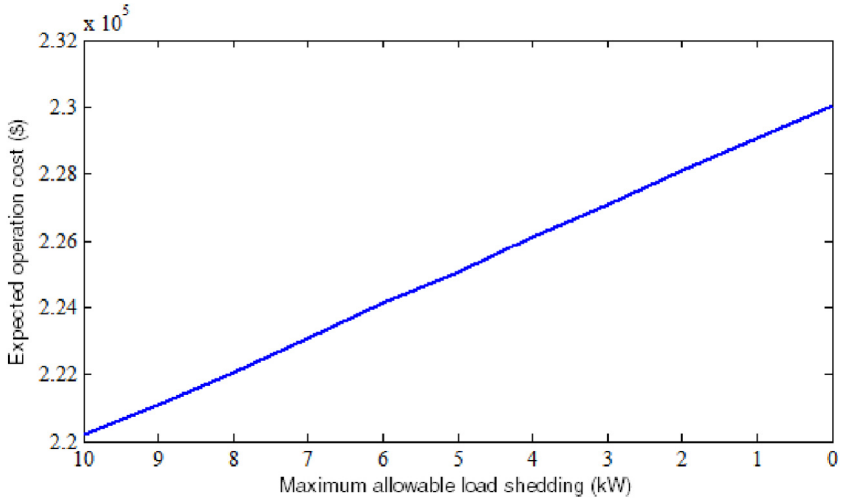

Fig. 20. Expected operation cost with respect to maximum allowable load shedding.

Table 5
Scheduling results of the MG in scenario 6.

Hour	P^L (kW)	P^{PV} (kW)	P^{WT} (kW)	f (Hz)	P^{FR} (kW)	P^{NR} (kW)	LSH (kW)	$\sum_g P^{DG}$ (kW)	$\sum_g \frac{1}{n_g^{gain}}$ (kW/Hz)
1	330.30	0	112.84	59.79	20.91	-1.15	1.54	193.86	1036.95
2	290.00	0	60.73	59.78	21.02	-1.01	0	207.24	424.76
3	327.60	0	86.85	59.78	21.16	-1.15	13.33	205.22	191.66
4	314.00	0	86.58	59.94	5.92	-0.31	0	221.19	191.66
5	385.50	0	86.72	59.79	20.05	-1.28	0	277.45	880.40
6	299.25	0	72.51	60.06	-6.01	0.29	0	233.04	1006.07
7	383.35	0	137.56	59.78	21.08	-1.34	16.70	206.67	191.66
8	332.00	1.36	137.87	60.18	-8.86	1.04	0	202.67	1019.34
9	367.50	5.95	131.44	60.08	-8.99	0.55	0	239.65	191.66
10	467.40	17.00	82.39	59.81	18.05	-1.40	0	348.56	191.66
11	486.00	25.30	107.21	59.82	17.86	-1.44	0	334.19	191.66
12	539.30	32.62	84.10	59.84	15.60	-1.40	0	405.58	1010.15
13	605.00	32.62	153.14	59.84	15.26	-1.53	0	402.45	849.85
14	564.40	54.06	100.05	59.86	13.76	-1.29	0	395.24	191.66
15	475.00	70.71	128.25	60.15	-5.80	1.25	0	283.09	1017.88
16	524.24	62.90	70.99	60.12	-2.64	1.10	0	394.09	979.68
17	580.65	44.33	102.29	59.87	12.07	-1.16	0	420.80	929.73
18	730.00	56.10	67.57	59.90	9.51	-1.15	0	595.67	611.14
19	793.00	40.46	112.84	59.92	7.04	-0.93	0	631.73	1277.77
20	598.50	15.63	115.63	60.07	-7.79	0.77	0	475.80	1225.90
21	730.00	0	65.00	59.92	7.07	-0.86	0	657.07	562.83
22	564.00	0	104.78	59.88	11.33	-1.06	0	446.83	1277.77
23	454.10	0	96.72	60.12	-2.85	0.97	0	361.20	695.02
24	430.00	0	65.74	59.83	16.56	-1.18	0	346.52	310.36

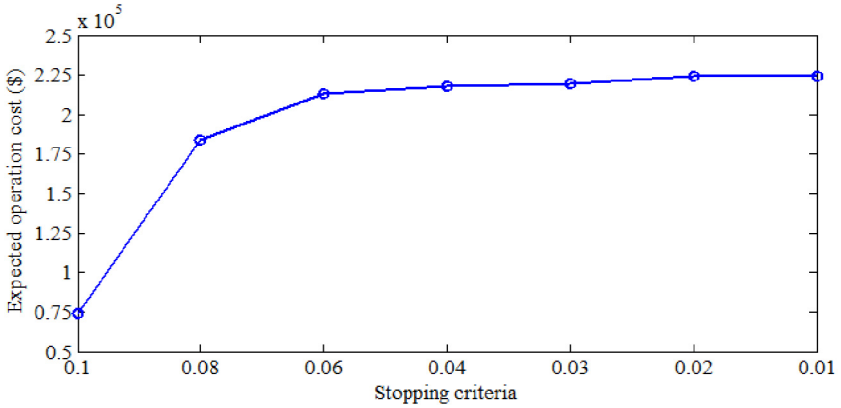

Fig. 21. The evolution of expected cost versus different stopping criteria.

thrifting was ensured by active participation of elastic frequency responsive loads in the primary level which was constructed on great potential capacity and high control flexibility of the proposed thermostatically controlled loads. The proposed load management module was conducted such a way not only it can become an effective provocation for end-user consumers to take part into microgrid energy management but it also can preserve the qualifying limitations of life comfort. As future perspectives, modeling the role of grid-forming renewable energy sources in coordinating with droop controlled DGs for providing more efficient primary frequency management structures can be an attractive subject. The proposed energy management system can also consider the potential of electric vehicles into the proposed demand responsiveloads.

Declaration of competing interest

The authors declare that they have no known competing financial interests or personal relationships that could have appeared to influence the work reported in this paper.

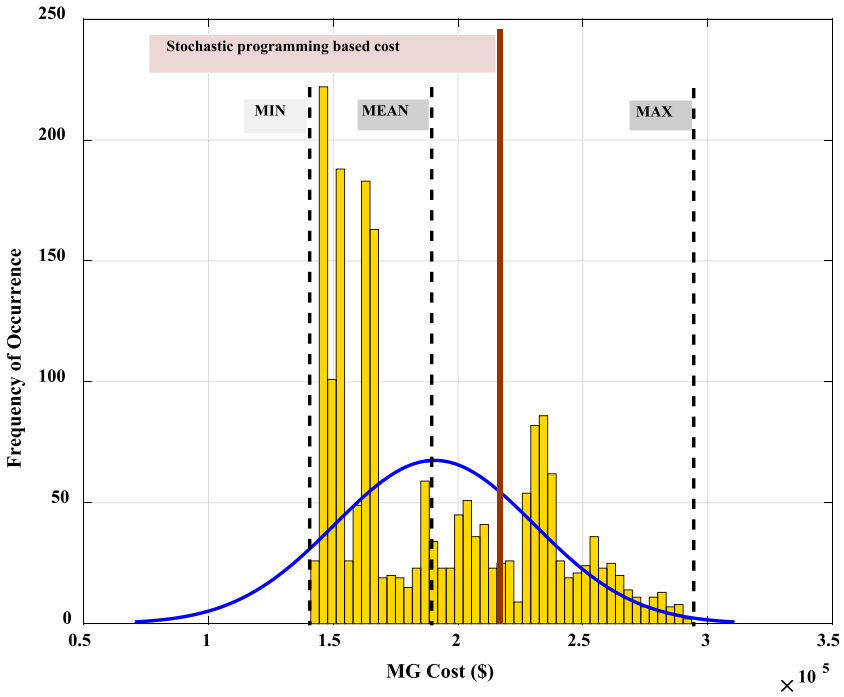

Fig. 22. Monte-Carlo Simulation histogram and comparison with stochastic programming.

CRediT authorship contribution statement

Navid Rezaei: Writing- original draft, Writing - review & editing, Software, Supervision. **Mohammadreza Mazidi:** Methodology, Investigation, Data curation. **Mehrdad Gholami:** Visualization, Resources. **Maryam Mohiti:** Conceptualization, Formal analysis, Validation.

References

Abdelaziz, M.M.A., El-Saadany, E.F., 2015. Economic droop parameter selection for autonomous microgrids including wind turbines. Renew. Energy 82, 108–113, 2015/10/01/.

Abdelaziz, M.M.A., Farag, H.E., El-Saadany, E.F., 2014. Optimum droop parameter settings of islanded microgrids with renewable energy resources. IEEE Trans. Sustain. Energy 5, 434–445.

Abdelaziz, M.M.A., Farag, H.E., El-Saadany, E.F., Mohamed, Y.A.-R.I., 2012. A novel and generalized three-phase power flow algorithm for islanded microgrids using a newton trust region method. IEEE Trans. Power Syst. 28, 190–201.

Abedini, M., Abedini, M., 2018. Energy management and control policies of the islanded microgrids. Sustainable Cities Soc. 38, 714–722, 2018/04/01/.

Amjady, N., Aghaei, J., Shayanfar, H.A., 2009. Stochastic multiobjective market clearing of joint energy and reserves auctions ensuring power system security. IEEE Trans. Power Syst. 24, 1841–1854.

Anon, 2014. IEEE standard for interconnecting distributed resources with electric power systems - amendment 1. In: IEEE Std 1547a-2014 (Amendment to IEEE Std 1547-2003). pp. 1–16.

Aunedi, M., Kountouriotis, P.-A., Calderon, J.O., Angeli, D., Strbac, G., 2013. Economic and environmental benefits of dynamic demand in providing frequency regulation. IEEE Trans. Smart Grid 4, 2036–2048.

Bidram, A., Davoudi, A., 2012. Hierarchical structure of microgrids control system. IEEE Trans. Smart Grid 3, 1963–1976.

Eid, B.M., Rahim, N.A., Selvaraj, J., El Khateb, A.H., 2014. Control methods and objectives for electronically coupled distributed energy resources in microgrids: A review. IEEE Syst. J. 10, 446–458.

Elizondo, J., Zhang, R.Y., Huang, P., White, J.K., Kirtley, J.L., 2016. Inertial and frequency response of microgrids with induction motors. In: 2016 IEEE 17th Workshop on Control and Modeling for Power Electronics (COMPEL). pp. 1–6.

Farzin, H., Fotuhi-Firuzabad, M., Moeini-Aghtaie, M., 2017. Stochastic energy management of microgrids during unscheduled islanding period. IEEE Trans. Ind. Inf. 13, 1079–1087.

The General Algebraic Modeling System (GAMS) Software. Available at: <http://www.gams.com>.

Ghofrani, A., Nazemi, D., Jafari, M.A., 2019. HVAC Load Synchronization in Smart Building Communities. Sustainable Cities and Society, 101741, 2019/08/01/.

Gholami, A., Sun, A., 2018. Towards resilient operation of multi-microgrids: An MISOCP-based frequency-constrained approach. IEEE Trans. Control Netw. Syst. 1.

Growe-Kuska, N., Heitsch, H., Romisch, W., 2003. Scenario reduction and scenario tree construction for power management problems. In: 2003 IEEE Bologna Power Tech Conference Proceedings, Vol. 3. p. 7.

Guerrero, J.M., Chandorkar, M., Lee, T., Loh, P.C., 2013. Advanced control architectures for intelligent microgrids—Part I: Decentralized and hierarchical control. IEEE Trans. Ind. Electron. 60, 1254–1262.

Gupte, A., Ahmed, S., Cheon, M.S., Dey, S., 2013. Solving mixed integer bilinear problems using MILP formulations. SIAM J. Optim. 23, 721–744.

Izadkhast, S., Garcia-Gonzalez, P., Frias, P., Bauer, P., 2017. Design of plug-in electric vehicle's frequency-droop controller for primary frequency control and performance assessment. IEEE Trans. Power Syst. 32, 4241–4254.

Khaledian, A., Ahmadian, A., Aliakbar-Golkar, M., 2017. Optimal droop gains assignment for real-time energy management in an islanding microgrid: a two-layer techno-economic approach. IET Gener. Transm. Distrib. 11, 2292–2304.

Li, Z., Zang, C., Zeng, P., Yu, H., Li, S., 2016. Agent-based distributed and economic automatic generation control for droop-controlled AC microgrids. IET Gener. Transm. Distrib. 10, 3622–3630.

Liu, J., Chen, H., Zhang, W., Yurkovich, B., Rizzoni, G., 2016. Energy management problems under uncertainties for grid-connected microgrids: A chance constrained programming approach. IEEE Trans. Smart Grid 8, 2585–2596.

Marzband, M., Ghazimirsaeid, S.S., Uppal, H., Fernando, T., 2017. A real-time evaluation of energy management systems for smart hybrid home microgrids. Electr. Power Syst. Res. 143, 624–633, 2017/02/01/.

Marzband, M., Sumper, A., Domínguez-García, J.L., Gumara-Ferret, R., 2013. Experimental validation of a real time energy management system for microgrids in islanded mode using a local day-ahead electricity market and MINLP. Energy Convers. Manage. 76, 314–322, 2013/12/01/.

Mazidi, M., Monsef, H., Siano, P., 2016. Design of a risk-averse decision making tool for smart distribution network operators under severe uncertainties: An IGDT-inspired augment ε-constraint based multi-objective approach. Energy 116, 214–235, 2016/12/01/.

Mazidi, M., Rezaei, N., Ghaderi, A., 2019. Simultaneous power and heat scheduling of microgrids considering operational uncertainties: A new stochastic p-robust optimization approach. Energy 185, 239–253, 2019/10/15/.

Mazidi, M., Zakariazadeh, A., Jadid, S., Siano, P., 2014. Integrated scheduling of renewable generation and demand response programs in a microgrid. Energy Convers. Manage. 86, 1118–1127, 2014/10/01/.

Molina-Garcia, A., Bouffard, F., Kirschen, D.S., 2011. Decentralized demand-side contribution to primary frequency control. IEEE Trans. Power Syst. 26, 411–419.

Pourghasem, P., Sohrabi, F., Abapour, M., Mohammadi-Ivatloo, B., 2019. Stochastic multi-objective dynamic dispatch of renewable and CHP-based islanded microgrids. Electr. Power Syst. Res. 173, 193–201, 2019/08/01/.

Raj, C.D., Gaonkar, D.N., Guerrero, J.M., 2018. Improved $P-f/Q-V$ and $P-V/Q-f$ droop controllers for parallel distributed generation inverters in AC microgrid. Sustainable Cities Soc. 41, 421–442, 2018/08/01/.

Rezaei, N., Ahmadi, A., Khazali, A.H., Guerrero, J.M., 2018. Energy and frequency hierarchical management system using information gap decision theory for islanded microgrids. IEEE Trans. Ind. Electron. 65, 7921–7932.

Rezaei, N., Kalantar, M., 2014. Economic–environmental hierarchical frequency management of a droop-controlled islanded microgrid. Energy Convers. Manage. 88, 498–515.

Rezaei, N., Kalantar, M., 2015a. Hierarchical energy and frequency security pricing in a smart microgrid: An equilibrium-inspired epsilon constraint based multi-objective decision making approach. Energy Convers. Manage. 98, 533–543, 2015/07/01/.

Rezaei, N., Kalantar, M., 2015b. Smart microgrid hierarchical frequency control ancillary service provision based on virtual inertia concept: An integrated demand response and droop controlled distributed generation framework. Energy Convers. Manage. 92, 287–301.

Samarakoon, K., Ekanayake, J., Jenkins, N., 2012. Investigation of domestic load control to provide primary frequency response using smart meters. IEEE Trans. Smart Grid 3, 282–292.

Simpson-Porco, J.W., Dörfler, F., Bullo, F., 2017. Voltage stabilization in microgrids via quadratic droop control. IEEE Trans. Automat. Control 62, 1239–1253.

Singh, S., Jagota, S., Singh, M., 2018. Energy management and voltage stabilization in an islanded microgrid through an electric vehicle charging station. Sustainable Cities Soc. 41, 679–694, 2018/08/01/.

Vahedipour-Dahraie, M., Rashidizadeh-Kermani, H., Najafi, H.R., Anvari-Moghaddam, A., Guerrero, J.M., 2017. Stochastic security and risk-constrained scheduling for an autonomous microgrid with demand response and renewable energy resources. IET Renew. Power Gener. 11, 1812–1821.

Wang, M.Q., Gooi, H., 2011. Spinning reserve estimation in microgrids. IEEE Trans. Power Syst. 26, 1164–1174.

Wu, L., Shahidehpour, M., Li, T., 2007. Stochastic security-constrained unit commitment. IEEE Trans. Power Syst. 22, 800–811.

Xu, Z., Ostergaard, J., Togeby, M., 2011. Demand as frequency controlled reserve. IEEE Trans. Power Syst. 26, 1062–1071.

Zakariazadeh, A., Jadid, S., Siano, P., 2014. Economic-environmental energy and reserve scheduling of smart distribution systems: A multiobjective mathematical programming approach. Energy Convers. Manage. 78, 151–164, 2014/02/01/.

Zhang, C., Xu, Y., Dong, Z.Y., Wong, K.P., 2017. Robust coordination of distributed generation and price-based demand response in microgrids. IEEE Trans. Smart Grid 9, 4236–4247.

Zia, M.F., Elbouchikhi, E., Benbouzid, M., Guerrero, J.M., 2019. Energy management system for an islanded microgrid with convex relaxation. IEEE Trans. Ind. Appl. 1.